World Applied Sciences Journal 28 (12): 2288-2301, 2013
ISSN 1818-4952

DOI: 10.5829/idosi.wasj.2013.28.12.84173

Well Log Analysis and Hydrocarbon Potential of the Khoman Formation, GPT Field, Northern Western Desert, Egypt

Ali Younis Ahmed Abdel-Rahman

Department of Geophysical Sciences, National Research Centre, Giza, Egypt

Abstract: The Khoman Formation is mainly made up of carbonate sediments with bands of shale, that constitute a gas reservoir in the GPT Field, Northern Western Desert, Egypt. Several vertical wells have been drilled and penetrated these sequences. Computer-assisted log analyses were used to evaluate the petrophysical parameters, such as shale volume, total porosity, effective porosity, water saturation, hydrocarbon saturation, flushed-zone saturation and reservoir and pay flags. Cross-plots of the petrophysical parameters versus depth were illustrated. Moreover, the cross-plots were used to show the lithologic and mineralogic components. On the basis of petrophysics data, the rocks of Khoman Formation are interpreted to be of good quality reservoir rocks, which have been confirmed with high effective porosity of about 27 % and high hydrocarbon saturation exceeding 62 %. The Khoman Formation reveals promising reservoir characteristics, especially in the central part of the study area, which should be taken into consideration during the future development of the gas field area.

Key words: Well logs · Hydrocarbon potential · Khoman Formation · GPT Field · Egypt

INTRODUCTION

The GPT Field in Abu Sannan area, which was discovered in 1983, has been put on production since March 1990 from three gas-producing reservoirs; these are Abu Roash "B", Abu Roash "D" and Bahariya. In 1992, the new Khoman gas reservoir was tested at commercial gas rates for the first time in Egypt [1]. Well log analysis and interpretation are the most important tasks to detect reservoir petrophysical parameters, such as porosity, water saturation and locating hydrocarbon zones Schlumberger [2]. One of the features of modern log interpretation is the systematic use of the computer, which allows a detailed analysis of the formations, through which the well had been drilled and can also be used to identify the depth and thicknesses of productive zones, to distinguish between oil, gas and water in a reservoir and to estimate hydrocarbon reserves [3]. An essential step in the formation evaluation process is the determination of the amount of shale present in the formation, because it is necessary to calculate formation porosity and fluid content[4].The Khoman chalky limestones constitute a gas reservoir (3 - 60 m pay with 10 - 30% porosity) fractured on the folds of the GPT, GPA and GPY fields in the Abu Gharadig Basin [5]. The study area is located in Abu Sennan concession within Abu El-Gharadig basin in the northern part of the Western Desert. It is approximately bounded by longitudes 28° 00' and 29° 00' E and by latitudes 29° 00' and 30° 00' N (Fig. 1). The present work deals with the detailed evaluation of the reservoir petrophysical characteristics, to evaluate the hydrocarbon potential of the Khoman reservoir in the GPT Field, using the geological and well logging data extracted from 20 wells, namely, GPT- 1 to 20. The open-hole well logging data include resistivity logs, gamma-ray, bulk density, neutron porosity, sonic transit-time and caliper, which have been measured by Schlumberger Company.

General Geology

Khoman Formation (Santonian-Maastrichtian): The Khoman Formation was deposited in deep open marine to outer shelf conditions. It overlies unconformably different members of the Abu Roash Formation, particularly in the structurally highest areas [6]. This section is characterized by low permeability.

Corresponding Author: Ali Younis Ahmed Abdel-Rahman, Department of Geophysical Sciences, National Research Centre, Giza, Egypt.

The top and base of Khoman Formation are marked by two regional unconformities. The study of the palynomorphs and planktonic foraminifera proves the existence of a regional hiatus between the Khoman Formation and the underlying Abu Roash Formation [7] and Schrank and Ibrahim [8]. The amount of unconformity depended on the position on the structural and/or topographic high and the magnitude of the uplift [9-12]. The Khoman Formation exhibits a marked change in facies, showing two main lithologic units (Khoman "A and B"). Earliest sediments are composed of interbedded shales and tight highly argillaceous limestones with rare sand intervals, Khoman "B" Member. This sequence is overlain by massive fine-grained, white chalky limestone with cherty bands, Khoman "A" Member, that frequently argillaceous in the lower part [13].

According to Ibrahim [14], the Khoman "A" Member is subdivided into three lithogenetic units, an upper argillaceous; a middle dolomitized chalky and a lower chalky. The dolomitization of the middle subunit played a great role in the accumulation of hydrocarbons, especially at the GPT-structure. This subunit is characterized by its fractured nature at the Abu Sennan high. The type section is the scarp of Ain Khoman to the southwest of Bahariya Oasis (27° 55' N, 28° 30' E).

The thickness map of Khoman Formation (Fig. 2) indicates that, the thickness increases outwards (basinal areas), which reflects a significant change in the structural pattern before the deposition of the Khoman Formation. The thickness is ranging from 78.5 m (in GPT- 16 well) to 290 m (in GPT- 8 well). The thinnest part of the formation is located around the wells: GPT- 20, 16, 19&17, indicating the presence of a ridge at that time at this part of the field. This ridge extends rather NE-SW. The structure contour map on the top of Khoman Formation (Fig. 3) reflects an elongated domal feature; having its apex centered at GPT- 1, 9, &16 wells. In the study area, the Khoman Formation was encountered at depths ranged between 1071 m (in GPT- 1 well) and 1213 m (in GPT- 15 well). The depths to the top surface of the Khoman Formation increase generally towards the flanks of the area with the deepest value in the NE direction.

MATERIALS AND METHODS

Twenty wells have been selected for investigating the Upper Cretaceous Khoman reservoir rocks, to evaluate the hydrocarbon potentiality in the study area. Open-hole 1og data including the traditional tools, such as resistivity logs, compensated neutron porosity, formation density compensated, borehole compensated sonic, photoelectric formation, caliper and gamma-ray for the studied unit were collected and digitized. The data should be corrected to different environmental effects. This study has been carried out through qualitative and quantitative analyses by means of the Interactive Petrophysics (IP) program. Cross-plots were used to show the lithologic and mineralogic components of the Khoman reservoir. The shale content was calculated from gamma ray, neutron, neutron-density and resistivity logs. The minimum shale content given by these shale indicators is likely to be close to the actual value of the shale content. The corrected porosity was estimated using a combination of the density and neutron logs, after applying various corrections. The water saturation was computed with Indonesian equation. Corrected well logs and reservoir parameters, which are derived from them, are plotted versus depth, including the vertical cross-plots and lithology identification cross-plots. These cross-plots give a quick view about the rock and mineral contents in a qualitative way. Some of these cross-plots give the amount of lithologic contents in a quantitative way. Such cross-plots are neutron-bulk density, gamma ray-bulk density and M–N cross-plots.

RESULTS AND DISCUSSIONS

Lithologic Interpretation with Cross-Plots: The identification of the matrix components is well defined through different cross-plots, where different types of matrix appear by combining different well logs. These cross-plots of the Khoman reservoir in the GPT Field can be illustrated as follows:

Neutron-Bulk Density Cross-Plot: The cross-plot of neutron-bulk density (Fig. 4) shows that, the main lithology is carbonates (limestone and dolomite) with shale. The sandstone content is generally low, as shown from the lesser plotted points along the sandstone line in this cross-plot.

Gamma-Ray-Bulk Density Cross-Plot: This plot (Fig. 5) reflects the scattering of plotted points, which means the variation of lithology of this rock unit. Points having low gamma-rays and low bulk densities indicate the presence of limestone and dolomite, points having medium gamma-rays and medium bulk densities indicate sandstone and points having high gamma-rays and high bulk densities reflect the abundance of shale.

By combination, it is clear that, the main lithology is the limestone and dolomite with shale and a few amount of sandstone.

Gamma-Ray-Neutron Cross-Plot: In the neutron-gamma-ray cross-plot, medium gamma-ray (40 - 55 API) and neutron porosity indicate shaly sandstone, while high gamma-ray (greater than 55 API) and high neutron porosity suggest rich shale (Rider [15]) and all points go up with the decrease of shale content, which is agreed with the results from neutron - bulk density (Fig. 6).

M–N Cross-Plot: The M–N cross-plots (Fig. 7) reveal the predominance of carbonate minerals (calcite), where the corresponding points are shifted towards the sandstone area. Finally, we can conclude that, the lithology of this reservoir from this cross-plot shows that, the main lithology is limestone and dolomite with shale and sandstone (Fig. 4 - 7). The carbonate content is generally high as shown from the highest plotted points along the limestone and dolomite lines in those cross-plots (Fig. 4-7).

Shale Type and Types of Porosity Cross-Plots: The neutron porosity and density porosity cross-plot can be used as a tool for the identification of shale content type in the rock unit, as investigated by Brook [16]. The dia porosity between neutron and density porosities cross-plot (Fig. 8) reveals high dispersed and low laminated habits of the intercalated shale and organic matter (ORG) effect. The (neutron-density) porosity and (sonic) porosity cross-plot (Fig. 9) is used for the determination of the type of reservoir porosity (primary or secondary) in the evaluated zones [17]. This cross-plot indicates the dominance of the high secondary porosity with low primary (inter-granular) porosity type.

Hydrocarbon Potential: Evaluation of the oil potential of the reservoir rocks is based on the results of well logging analysis carried out for the wells in the study area. The analysis includes vertical petrophysical distribution cross-plots of the analyzed data in each well and the horizontal iso-parametric configuration maps [18, 19] Asquith and Krygowski [3].

Vertical Distribution of Hydrocarbon Occurrences: Vertical distributions of the hydrocarbon occurrences are illustrated through the litho-saturation cross-plots.Litho-saturation cross-plots are very important in well log interpretation. It can be used for the illustration of the gross character of the petrophysical parameters, in terms of lithology fractionation and fluid saturations; such as water and hydrocarbon saturations. Formation analysis includes total, effective porosities and matrix content (sandstone, limestone and dolomite) in 100 % scale. Moreover, caliper, neutron and density logs were presented in order to continuously check the reliability of the data encountered and their corresponding false petrophysical parameters analysis [18].

These litho-saturation cross-plots of the Khoman reservoir in the upper Cretaceous sequences of the 20 wells of GPT field are interpreted. The evaluation of the concerned Khoman reservoir in GPT- 9, 11, 10 and 13 wells are given here (Figs. 10 - 13), as an example of the other studied wells. In these wells, the rock units are composed of high percent of limestone, followed by shale with low amounts of sandstone and dolomite contents. The shale content is represented by low values ranging from zero (clean) in all wells to 41% in GPT- 13 well. The effective porosity of this reservoir rock ranges from 5 % (in GPT- 10 well) to 29 % (in GPT- 11 well), with remarkably high allover the unit in the studied wells. Gas is predominant along the unit and the water is represented by minor occurrences in GPT- 9 and 11 wells, whereas in GPT- 10 and 13 wells, the gas exhibited very minor traces. Based on the lithological, petrophysical and fluid analysis, the studied interval has been differentiated into reservoir and pay flags. From the above, the Khoman reservoir is of good reservoir quality that contains hydrocarbon and could be a gases producer from these studied wells.

Lateral Variations of Hydrocarbon Plays: The lateral variations of hydrocarbon can be studied through a number of shaliness, effective porosity and saturation maps. These maps utilize the important effect of some petrophysical parameters; such as shale content, effective porosity and water and hydrocarbon saturations. The study of these parameters, as available maps, is very essential for judging their lateral variation and the factors controlling such variations Asquith and Gibson [18], Rider, [19].

The Shale Content Contour Map: The shale content distribution of the Khoman reservoir (Fig. 14) shows an that, the maximum recorded shale content value is at GPT- 13 well of 25 % to the southwestern part and the minimum recorded one at GPT- 20 well of 10% at the central part of the study area. It is noteworthy that, the shale content of Khoman Formation generally increases outward of the flanks of the study area.

Effective Porosity Contour Map: This map (Fig. 15) denotes that, the effective porosity is well developed within the Khoman Formation, where it varies from 10 % (at GPT- 15 well) to 27 % (at GPT- 1 well). The general trend of porosity increasing is toward the central part of the study area, while the low porosity values occupy the flanks of the field area. Such a trend is nearly matching with the direction of shale change within the Khoman Formation. Also, comparing the structure contour map constructed on the top of Khoman Formation (Fig. 3), it can be noticed that, the highly porous area occupying the relatively high structural area lying at the central part of the study area.

Hydrocarbon Saturation Map: Figure (16) reflects a considerable gas saturation, where it varies from 2 % (at GPT- 13 well) to 62 % (at GPT- 9 well). The increasing trend is toward the high central parts (crest) of the field area, reflecting the migration of the gases up to these parts due to the inter-granular pore spaces and fractured nature at the Abu Sennan high.

Net Pay Map: Figure (17) indicates that, the net-pay thickness of gas within the Khoman Formation attains a thickness of 3 m (in GPT- 18 well) to 60 m (in GPT- 20 well). It is worth-mentioning that, the thickness of the net-pay is calculated by using certain cutoffs of: porosity >= 10 %, water saturation <= 50 % and clay volume <= 35 %). The net gases are concentrated in the central part of the study area.

CONCLUSIONS

Geological information and the results obtained from well log analysis in the GPT Field have been used to study and evaluate the petrophysical characteristics and hydrocarbon prospective of the Upper Cretaceous Khoman Formation. We conclude, from cross-plots analysis that, the lithology is dominated by thick porous limestone with little shale, sandstone and dolomite intercalations. The study area is an elongated domal feature; having its apex centered at GPT- 1, 9, &16 wells. Contour maps of the shale content, effective porosity, hydrocarbon saturation and net-pay show that, the reservoir parameters of GPT Field suggest a good reservoir within the Khoman Formation. The domal feature of this reservoir increases the hydrocarbon potentiality of GPT Field.

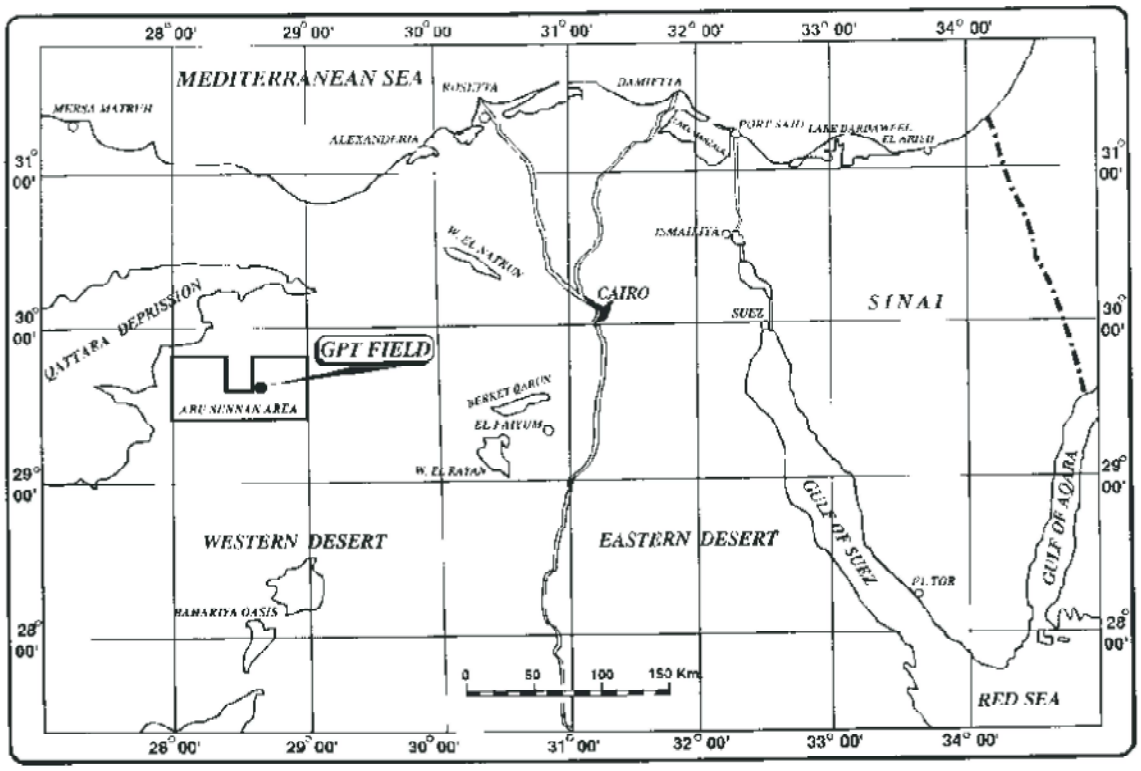

Fig. 1: Location map of the study area, Western Desert, Egypt.

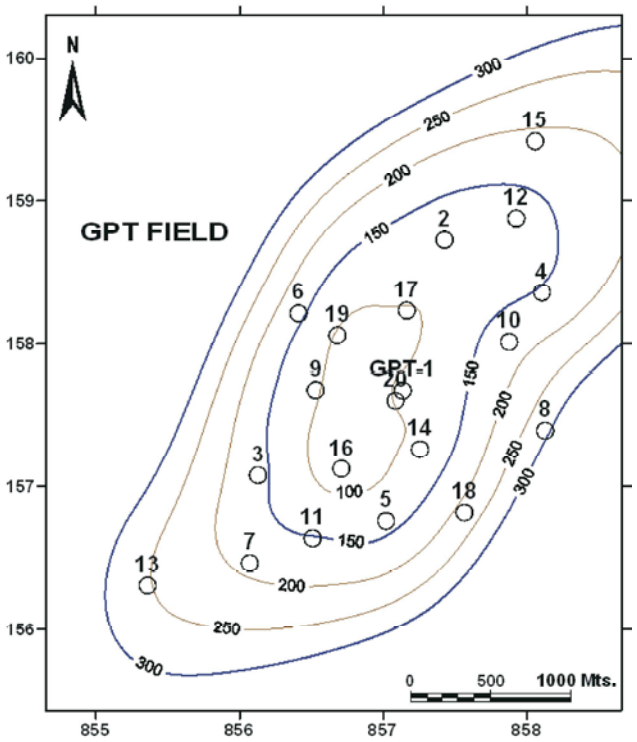

Fig. 2: Thickness contour map of the Khoman Formation, GPT Field, Abu Sannan Area, Western Desert, Egypt, (C.I. = 50 m.).

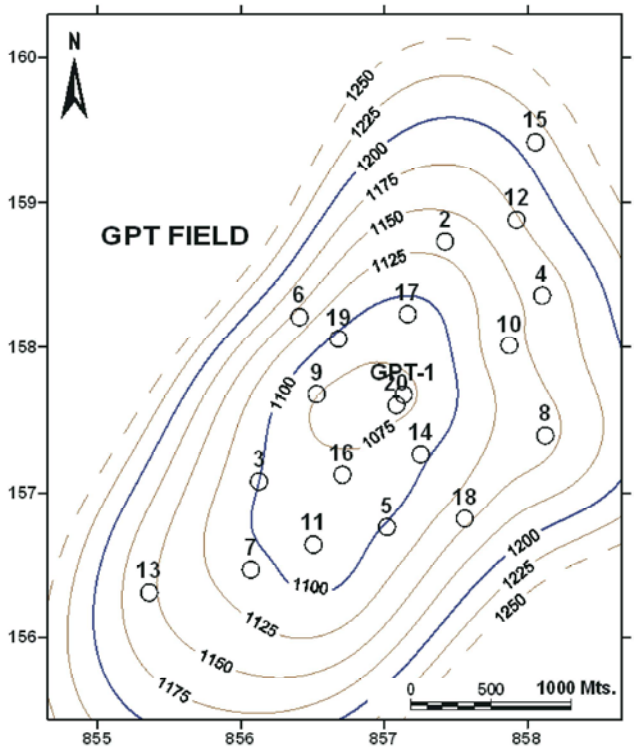

Fig. 3: Structure contour map on the top of Khoman Formation, GPT Field, Abu Sannan Area, Western Desert, Egypt, (C.I. = 25 m.).

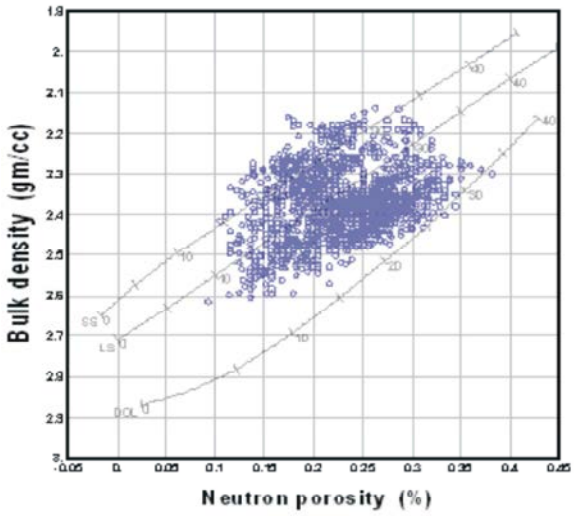

Fig. 4: Neutron porosity and bulk density crossplot of the Khoman Formation in the study area.

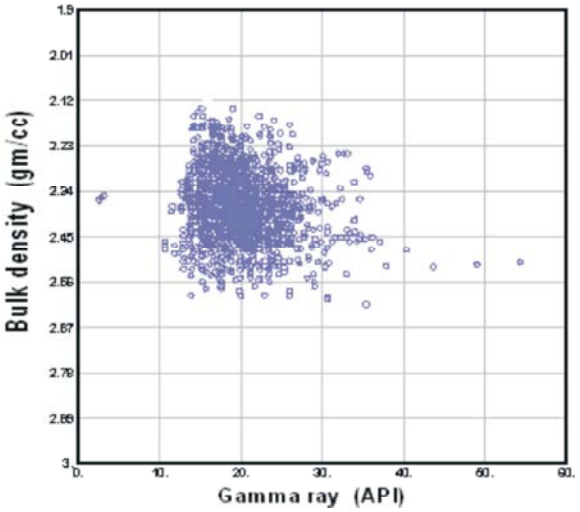

Fig. 5: Gamma ray and bulk density crossplot of the Khoman Formation in the study area.

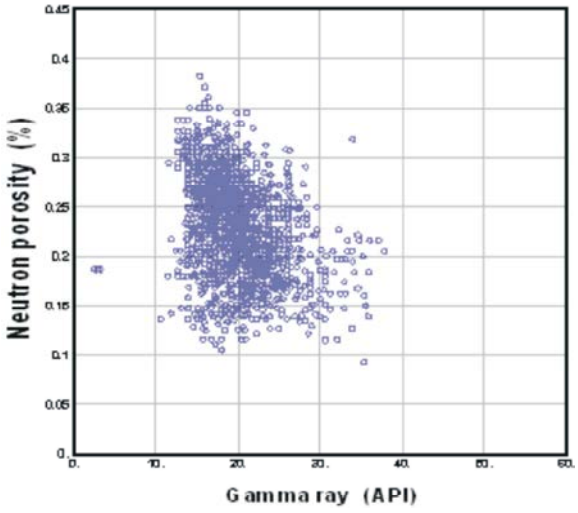

Fig. 6: Gamma ray and neutron porosity crossplot of the Khoman Formation in the study area.

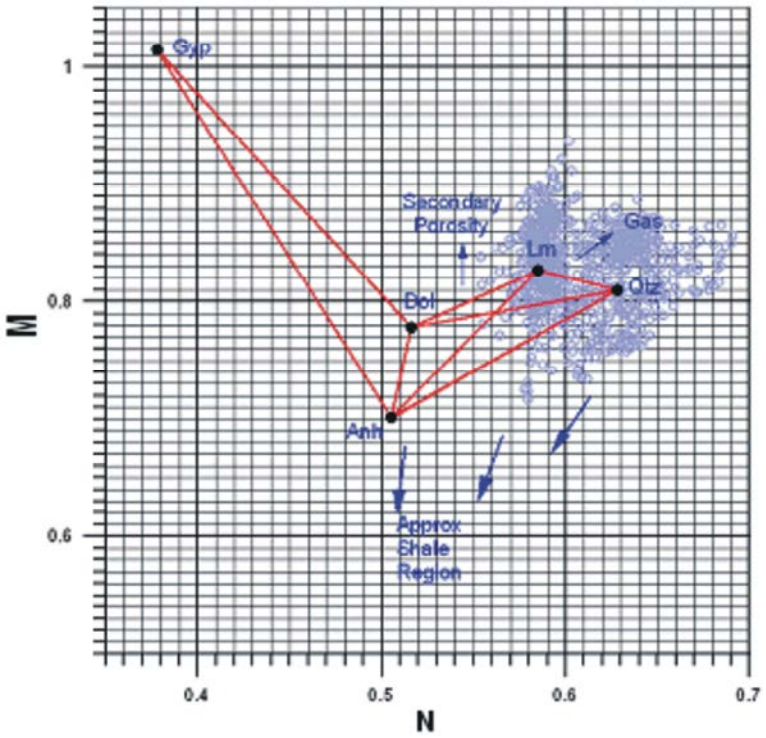

Fig. 7: M-N plot showing lithological components of the Khoman Formation in the study area.

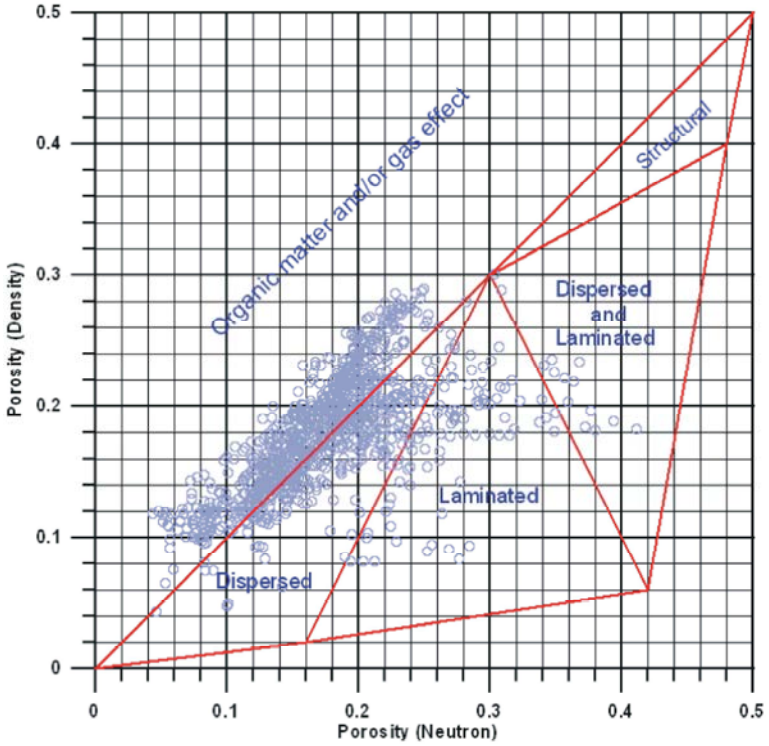

Fig. 8: Neutron porosity versus density porosity crossplot showing habitat of shale in the Khoman Formation in the study area.

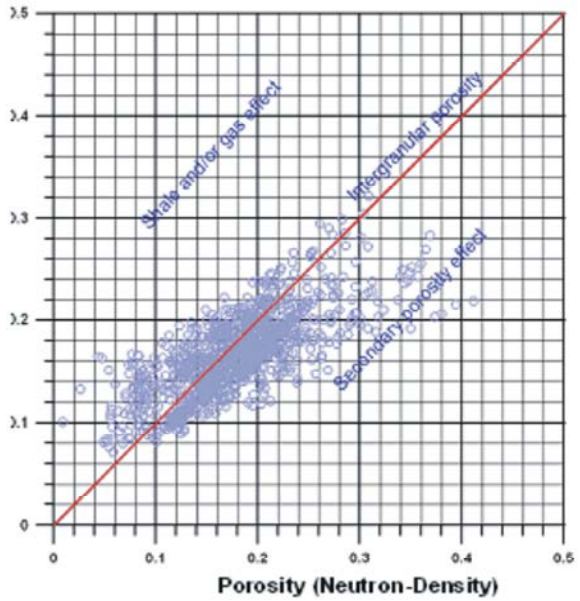

Fig. 9: Crossplot of porosity (neutron-density) versus porosity (sonic) showing type of porosity of the Khoman reservoir in the study area.

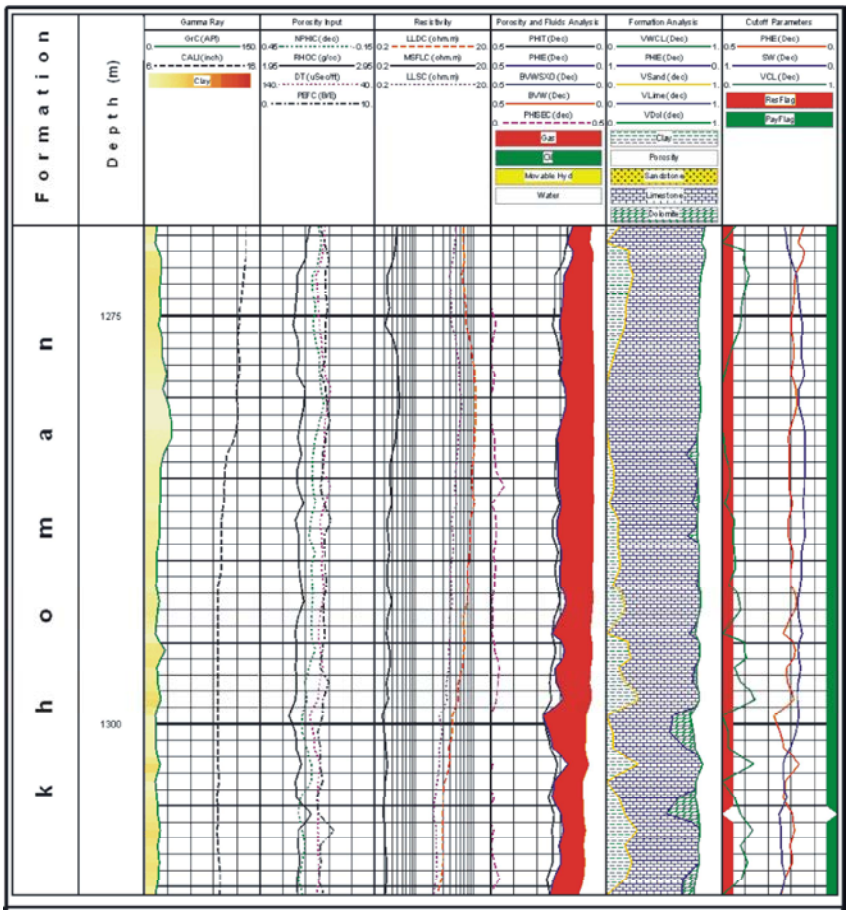

Fig. 10: The litho-saturation cross-plot illustrating variations in petrophysical characteristics of the Khoman Formation, GPT-9 well, Abu Sannan Area, Western Desert, Egypt.

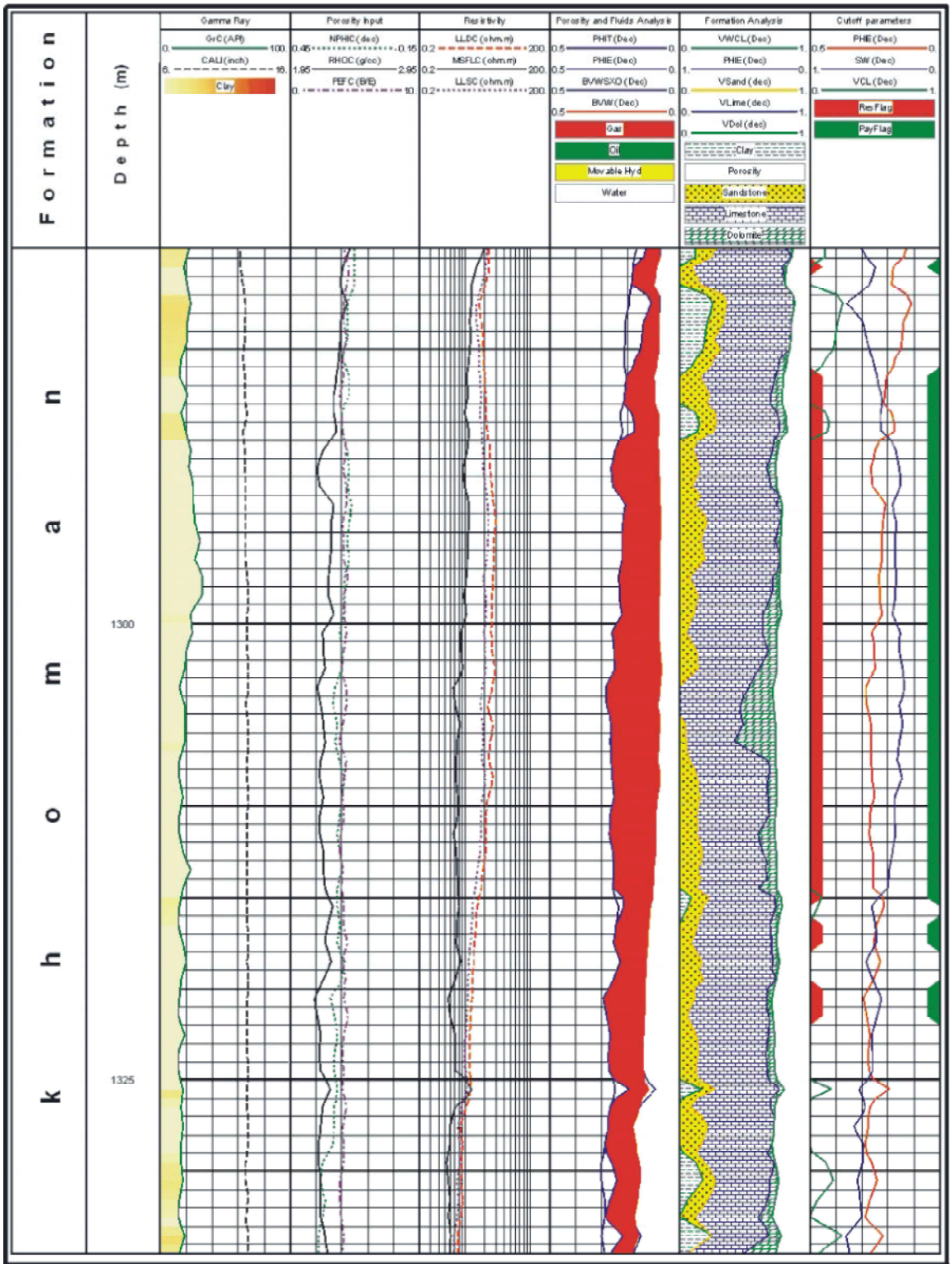

Fig. 11: The litho-saturation cross-plot illustrating vertical variations in petrophysical characteristics of the Khoman Formation, GPT-11 well, Abu Sannan Area, Western Desert, Egypt.

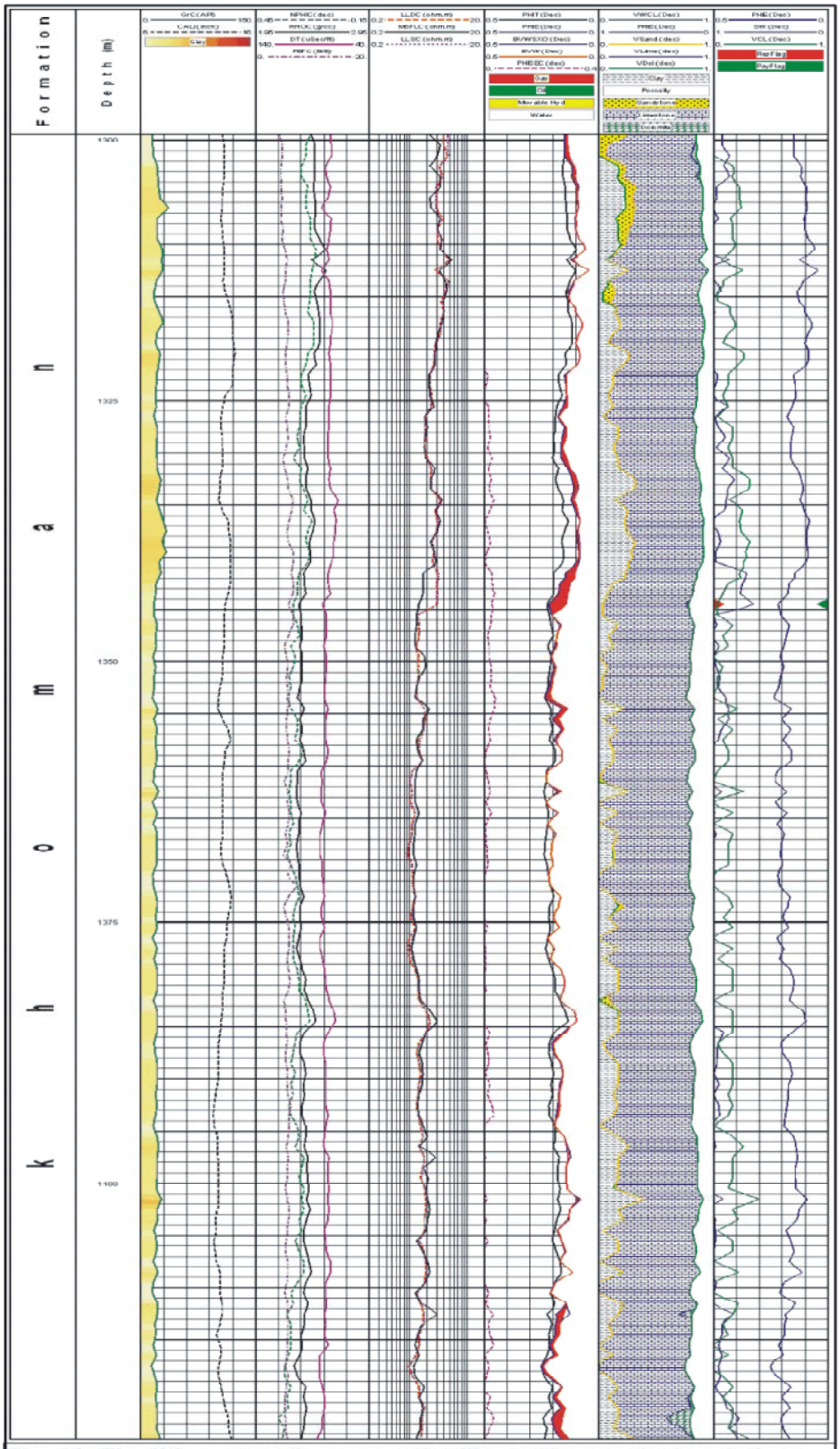

Fig. 12: The litho-saturation crossplot illustrating vertical variations in petrophysical characteristics of the Khoman Formation, GPT-10 well, Abu Sannan Area, Western Desert, Egypt.

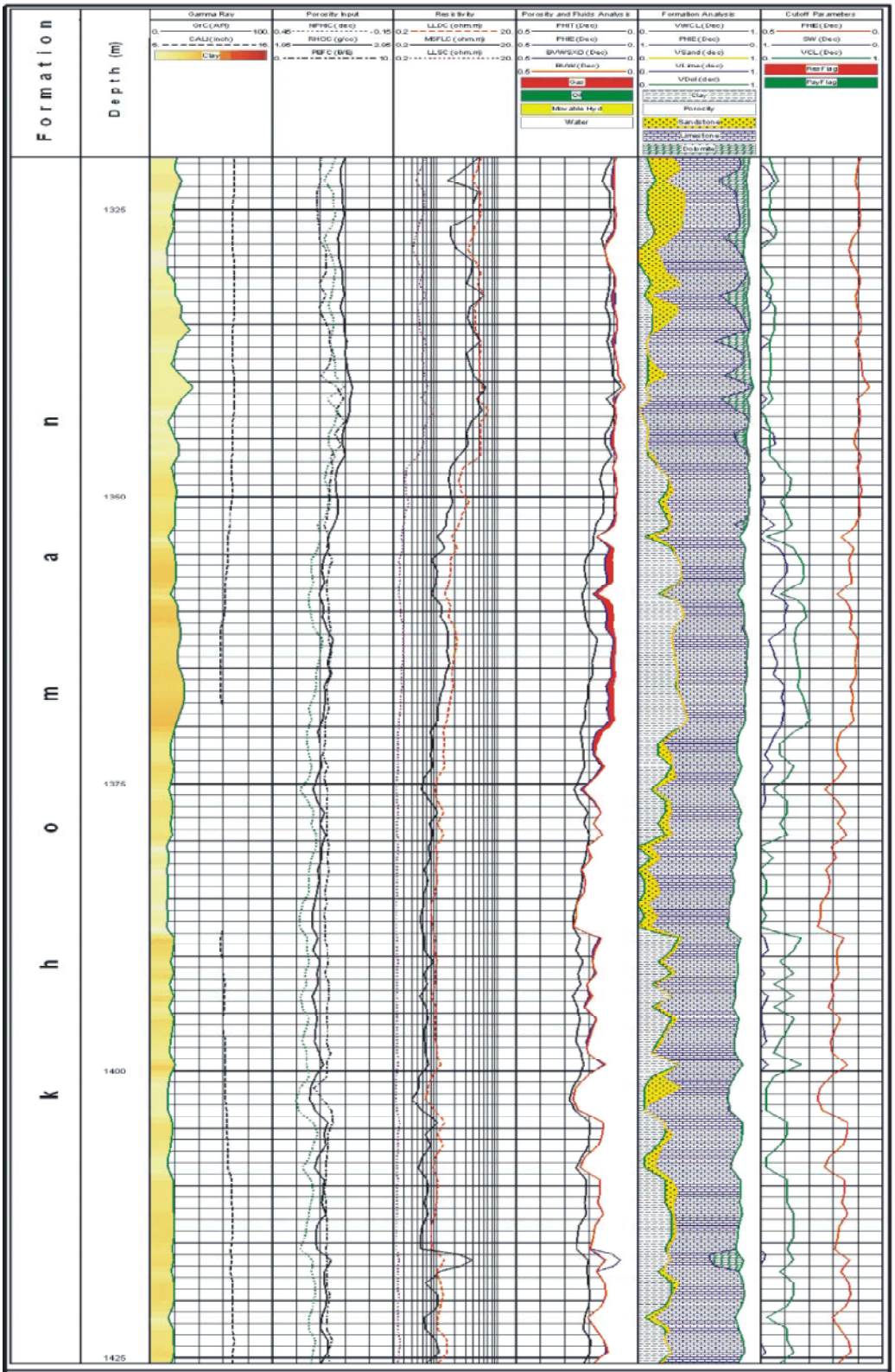

Fig. 13: The litho-saturation crossplot illustrating vertical variations in petrophysical characteristics of the Khoman Formation, GPT-13 well, Abu Sannan Area, Western Desert, Egypt.

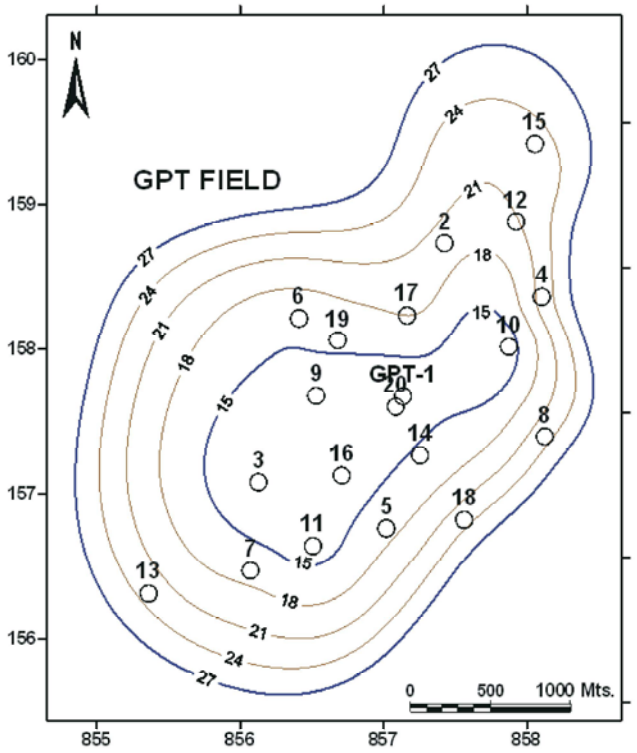

Fig. 14: Shale content contour map of the Khoman Formation, GPT Field, Abu Sannan Area, Western Desert, Egypt, (C.I. = 3%).

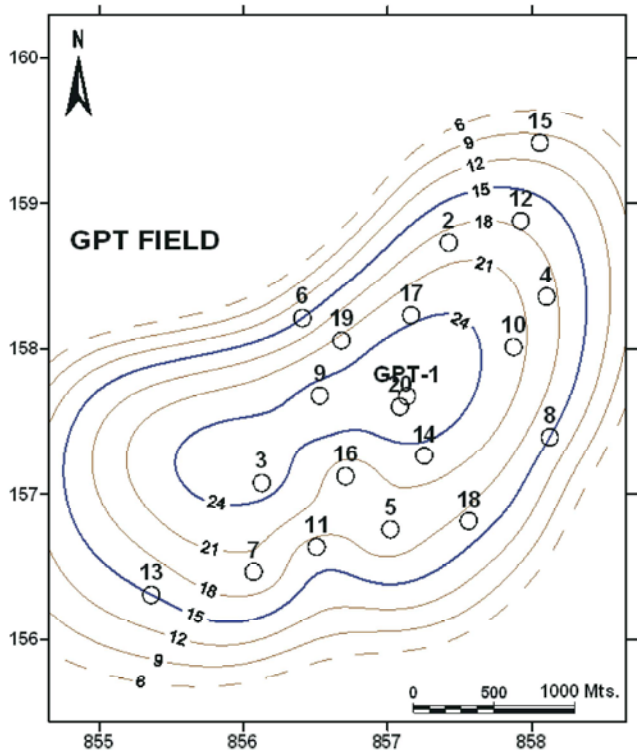

Fig. 15: Effective porosity contour map of the Khoman Formation, GPT Field, Abu Sannan Area, Western Desert, Egypt, (C.I. = 3%).

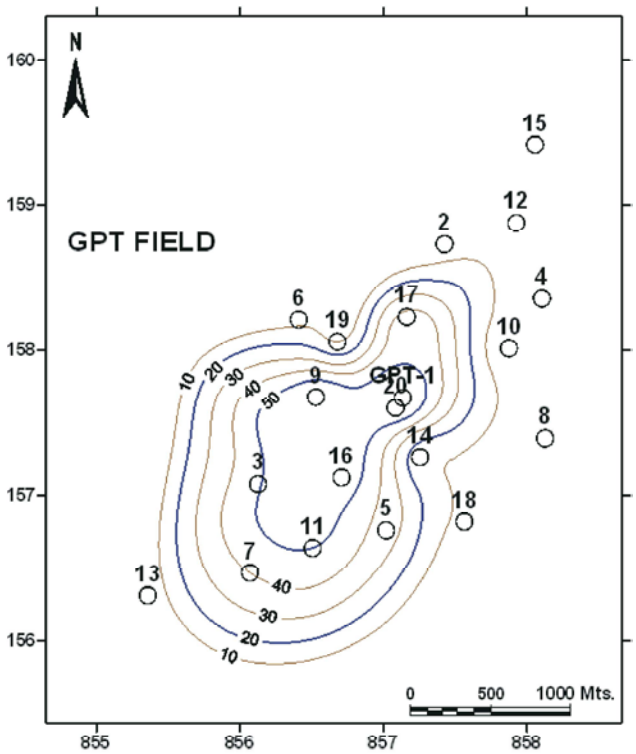

Fig. 16: Hydrocarbon saturation contour map of the Khoman Formation, GPT Field, Abu Sannan Area, Western Desert, Egypt, (C.I. = 10%).

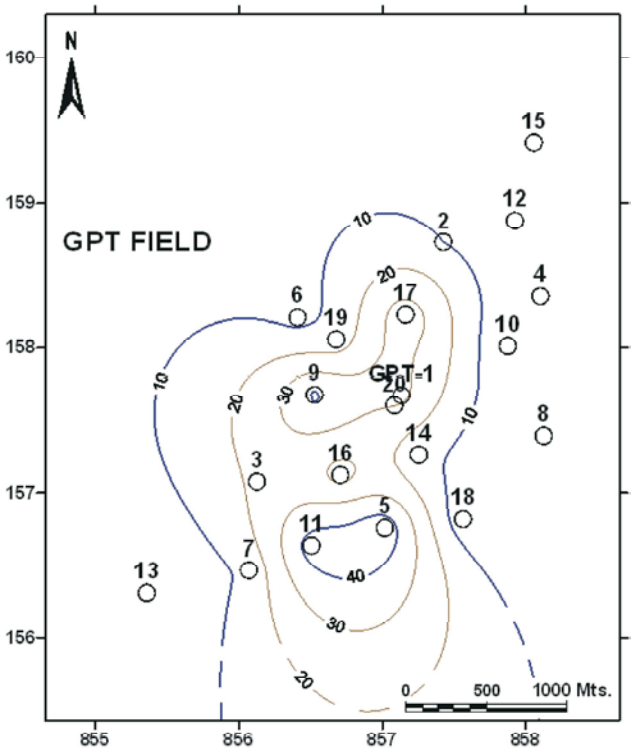

Fig. 17: Net pay thickness contour map of the Khoman Formation, GPT Field, Abu Sannan Area, Western Desert, Egypt, (C.I. = 10m.).

REFERENCES

1. Egyptian General Petroleum Corporation, E.G.P.C., 1992. In Western Desert, oil and gas fields, a comprehensive overview (pp. 1-431). Paper presented at the 11th Petroleum Exploration and Production Conference, Egyptian General Petroleum Corporation, Cairo.
2. Schlumberger, 1974. Log interpretation: V. 2 (Application). Schlumberger Limited, New York, pp: 116.
3. Asquith, G. and D. Krygowski, 2004. Basic well log analysis. American Association of Petroleum Geologists, Tulsa, pp: 244.
4. Kamel, M.H. and W.H. Mohamed, 2003. Estimation of shale volume using a combination of the three porosity logs. J. Pet. Sci. Eng., 40: 145-157.
5. Sestini, G., 1995. Egypt. In: H. Kulke, (Ed.), Regional petroleum geology of the world, part II: Africa, America, Australia and Antarctica (Vol. Beiträge zur egionalen Geologie der Erde, Band 22, pp: 66-87), Gebrüder Bornträger Verlagsbuchhandlung, Stuttgart.
6. Hantar, G., 1990. North Western Desert. In Said, R. (Ed.), Geology of Egypt (pp: 293-319), Balkema, Rotterdam.
7. Abd El Kireem, R.M. and A.I.M. Ibrahim, 1987. Late Cretaceous biostratigraphy and palaeobathymetry of the Betty well No.1, Western Desert, Egypt. In Matheis, G., Schandelmeir, H. (Ed.), Current Research African Earth Science (pp: 165-169), Balkema, Rotterdam.
8. Schrank, E. and A.I.M. Ibrahim, 1995. Cretaceous (Aptian-Masstrichtian) palynology of formaninifera dated wells (KRM-1, AG-18) in northwestern Egypt, with notes on Eocene dinoflagellates. Review Berliner Geowisenschaftliche Abhandlungen A177, pp: 1-44.
9. Hume, W.F., 1911. The effects of secular oscillations in Egypt during the Cretaceous and Eocene periods. 'Review Geological Society of London, 67: 118-148.
10. Shukri, N.M., 1954. Remarks on geological structure of Egypt. Review Soc. Geogr. Egypt Bull., 27: 65-82.
11. Amin, M.S., 1961. In Subsurface features and oil prospects of the Western Desert of Egypt (pp: 1-8). Paper presented at the 3rd Arab Petroleum Congress, Secretariat General League of Arab States, Alexandria, Egypt.
12. Said, R., 1962. Geology of Egypt. Amsterdam, Elsevier Science Publishing Company Inc., pp: 377.
13. Fawzy, A. and M. Dahi, 1992. In Regional geological evaluation of the Western Desert, Egypt. Paper presented at the Geology of the Arab World, Cairo University, pp: 111-149,
14. Ibrahim, M., 1992. Evaluation of hydrocarbon potentiality of Khoman Formation, Abu Sennan-Alan El Shawish Concession, western desert. 11th E.G.P.C. Expl. Conf. Cairo, 2: 16.
15. Rider, M.H., 1986. The geological interpretation of well logs. New York: John Wiley and Sons, Inc., pp: 175.
16. Brook, J., 1984. Analyzing your logs, V. II. Advanced open hole log interpretation. Petro-Media, Inc., Tyler.
17. Steiber, R.G., 1973. Optimization of shale volumes in open hole logs. J. Pet. Tech., 31: 147-162.
18. Asquith, G.B. and C.R. Gibson, 1997. Basic well log analysis for geologists. American Association of Petroleum Geologists, Tulsa, pp: 215.
19. Rider, M.H., 2000. The geological interpretation of well logs. Rider French Consulting Ltd., Southerland, pp: 280.